

Chapter 27

Extreme States of Nuclear Matter: 1980

Johann Rafelski

Abstract The theory of hot nuclear fireballs consisting of all possible finite-size hadronic constituents in chemical and thermal equilibrium is presented. As a complement of this hadronic gas phase characterized by maximal temperature and energy density, the quark bag description of the hadronic fireball is considered. Preliminary calculations of temperatures and mean transverse momenta of particles emitted in high multiplicity relativistic nuclear collisions together with some considerations on the observability of quark matter are offered.

27.1 Overview

I wish to describe, as derived from known traits of strong interactions, the likely thermodynamic properties of hadronic matter in two different phases: the hadronic gas consisting of strongly interacting but individual baryons and mesons, and the dissolved phase of a relatively weakly interacting quark-gluon plasma. The equations of state of the hadronic gas can be used to derive the particle temperatures and mean transverse momenta in relativistic heavy ion collisions, while those of the quark-gluon plasma are more difficult to observe experimentally. They may lead to recognizable effects for strange particle yields. Clearly, the ultimate aim is to understand the behaviour of hadronic matter in the region of the phase transition from gas to plasma and to find characteristic features which will allow its experimental observation. More work is still needed to reach this goal. This report is an account of my long and fruitful collaboration with R. Hagedorn [1].

Invited lecture at Quark Matter 1: *Workshop on Future Relativistic Heavy Ion Experiments* at the Gesellschaft für Schwerionenforschung (GSI), Darmstadt, Germany, 7–10 October 1980; circulated in the GSI81-6 Orange Report, pp. 282–324, R. Bock and R. Stock, editors; Reprinted in the ‘Bormio 1981’ Winter School proceedings. Presented here in complete original format omitting SBM pictures shown in previous chapters.

J. Rafelski (✉)

Department of Physics, University of Arizona, Tucson, AZ 85721, USA

© The Author(s) 2016

J. Rafelski (ed.), *Melting Hadrons, Boiling Quarks – From Hagedorn Temperature to Ultra-Relativistic Heavy-Ion Collisions at CERN*,

DOI 10.1007/978-3-319-17545-4_27

The theoretical techniques required for the description of the two phases are quite different: in the case of hadronic gas, a strongly attractive interaction has to be accounted for, which leads to the formation of the numerous hadronic resonances—which are in fact bound states of several (anti) quarks. If this is really the case, then our intuition demands that at sufficiently high particle (baryon) density the individuality of such a bound state will be lost. In relativistic physics in particular, meson production at high temperatures might already lead to such a transition at moderate baryon density. As is currently believed, the quark–quark interaction is of moderate strength, allowing a perturbative treatment of the quark-gluon plasma as relativistic Fermi and Bose gases. As this is a very well studied technique to be found in several reviews [2], we shall present the relevant results for the relativistic Fermi gas and restrict the discussion to the interesting phenomenological consequences. Thus the theoretical part of this report will be devoted mainly to the strongly interacting phase of hadronic gas. We will also describe some experimental consequences for relativistic nuclear collisions such as particle temperatures, i.e., mean transverse momenta and entropy.

As we will deal with relativistic particles throughout this work, a suitable generalization of standard thermodynamics is necessary, and we follow the way described by Touschek [3]. Not only is it the most elegant, but it is also by simple physical arguments the only *physical* generalization of the concepts of thermodynamics to relativistic particle kinematics. Our notation is such that $\hbar = c = k = 1$. The inverse temperature β and volume V are generalized to become four-vectors:

$$\begin{aligned} E &\longrightarrow p^\mu = (p^0, \mathbf{p}) = mu^\mu, & u_\mu u^\mu &= 1, \\ \frac{1}{T} &\longrightarrow \beta^\mu = (\beta^0, \boldsymbol{\beta}) = \frac{1}{T}v^\mu, & v_\mu v^\mu &= 1, \\ V &\longrightarrow V^\mu = (V^0, \mathbf{V}) = Vw^\mu, & w_\mu w^\mu &= 1, \end{aligned} \quad (27.1)$$

where u^μ , v^μ , and w^μ are the four-velocities of the total mass, the thermometer, and the volume, respectively. Usually, $\langle u^\mu \rangle = v^\mu = w^\mu$.

We will often work in the frame in which all velocities have a timelike component only. In that case we shall often drop the Lorentz index μ , as we shall do for the arguments $V = V_\mu$, $\beta = \beta_\mu$ of different functions.

The attentive reader may already be wondering how the approach outlined here can be reconciled with the concept of quark confinement. We will now therefore explain why the occurrence of the high temperature phase of hadronic matter—the quark-gluon plasma—is still consistent with our incapability to liberate quarks in high energy collisions. It is thus important to realize that the currently accepted theory of hadronic structure and interactions, quantum chromodynamics [4], supplemented with its phenomenological extension, the MIT bag model (for a review, see for example [5]), allows the formation of large space domains filled with (almost) free quarks. Such a state is expected to be unstable and to decay again into individual hadrons, following its free expansion. The mechanism of quark

confinement requires that all quarks recombine to form hadrons again. Thus the quark-gluon plasma may be only a transitory form of hadronic matter formed under special conditions and therefore quite difficult to detect experimentally.

We will recall now the relevant postulates and results that characterize the current understanding of strong interactions in quantum chromodynamics (QCD). The most important postulate is that the proper vacuum state in QCD is not the (trivial) perturbative state that we (naively) imagine to exist everywhere and which is little changed when the interactions are turned on/off. In QCD, the true vacuum state is believed to have a complicated structure which originates in the glue ('photon') sector of the theory. The perturbative vacuum is an excited state with an energy density \mathcal{B} above the true vacuum. It is to be found inside hadrons where perturbative quanta of the theory, in particular quarks, can therefore exist. The occurrence of the true vacuum state is intimately connected to the glue-gluon interaction. Unlike QED, these massless quanta of QCD, also carry a charge—colour—that is responsible for the quark-quark interaction.

In the above discussion, the confinement of quarks is a natural feature of the hypothetical structure of the true vacuum. If it is, for example, a colour superconductor, then an isolated charge cannot occur. Another way to look at this is to realize that a single coloured object would, according to Gauss' theorem, have an electric field that can only end on other colour charges. In the region penetrated by this field, the true vacuum is displaced, thus effectively raising the mass of a quasi-isolated quark by the amount $\mathcal{B}V_{\text{field}}$.

Another feature of the true vacuum is that it exercises a pressure on the surface of the region of the perturbative vacuum to which quarks are confined. Indeed, this is just the idea of the original MIT bag model [6]. The Fermi pressure of almost massless light quarks is in equilibrium with the vacuum pressure \mathcal{B} . When many quarks are combined to form a giant quark bag, then their properties inside can be obtained using standard methods of many-body theory [2]. In particular, this also allows the inclusion of the effect of internal excitation through a finite temperature and through a change in the chemical composition.

A further effect that must be taken into consideration is the quark-quark interaction. We shall use here the first order contribution in the QCD running coupling constant $\alpha_s(q^2) = g^2/4\pi$. However, as $\alpha_s(q^2)$ increases when the average momentum exchanged between quarks decreases, this approach will have only limited validity at relatively low densities and/or temperatures. The collective screening effects in the plasma are of comparable order of magnitude and should reduce the importance of perturbative contributions as they seem to reduce the strength of the quark-quark interaction.

From this general description of the hadronic plasma, it is immediately apparent that, at a certain value of temperature and baryon number density, the plasma must disintegrate into individual hadrons. Clearly, to treat this process and the ensuing further nucleonisation by perturbative QCD methods is impossible. It is necessary to find a semi-phenomenological method for the treatment of the thermodynamic system consisting of a gas of quark bags. The hadronic gas phase is characterized by those reactions between individual hadrons that lead to the formation of new

particles (quark bags) only. Thus one may view [7–9] the hadronic gas phase as being an assembly of many different hadronic resonances, their number in the interval $(m^2, m^2 + dm^2)$ being given by the mass spectrum $\tau(m^2, b)dm^2$. Here the baryon number b is the only discrete quantum number to be considered at present. All bag–bag interaction is contained in the mutual transmutations from one state to another. Thus the gas phase has the characteristic of an infinite component ideal gas phase of extended objects. The quark bags having a finite size force us to formulate the theory of an extended, though otherwise ideal multicomponent gas.

It is a straightforward exercise, carried through in the beginning of the next section, to reduce the grand partition function Z to an expression in terms of the mass spectrum $\tau(m^2, b)$. In principle, an experimental form of $\tau(m^2, b)$ could then be used as an input. However, the more natural way is to introduce the statistical bootstrap model [7], which will provide us with a theoretical τ that is consistent with assumptions and approximations made in determining Z .

In the statistical bootstrap, the essential step consists in the realization that a composite state of many quark bags is in itself an ‘elementary’ bag [1, 10]. This leads directly to a nonlinear integral equation for τ . The ideas of the statistical bootstrap have found a very successful application in the description of hadronic reactions [11] over the past decade. The present work is an extension [1, 9, 12] and application [1, 13] of this method to the case of a system containing any number of finite size hadronic clusters with their baryon numbers adding up to some fixed number. Among the most successful predictions of the statistical bootstrap, we record here the derivation of the limiting hadronic temperature and the exponential growth of the mass spectrum.

We see that the theoretical description of the two hadronic phases—the individual hadron gas and the quark-gluon plasma—is consistent with observations and with the present knowledge of elementary particles. What remains is the study of the possible phase transition between those phases as well as its observation. Unfortunately, we can argue that in the study of temperatures and mean transverse momenta of pions and nucleons produced in nuclear collisions, practically all information about the hot and dense phase of the collision is lost, as most of the emitted particles originate in the cooler and more dilute hadronic *gas* phase of matter. In order to obtain reliable information on quark matter, we must presumably perform more specific experiments. We will briefly point out that the presence of numerous \bar{s} quarks in the quark plasma suggest, as a characteristic experiment, the observation $\bar{\Lambda}$ hyperons.

We close this report by showing that, in nuclear collisions, unlike pp reactions, we can use equilibrium thermodynamics in a large volume to compute the yield of strange and anti-strange particles. The latter, e.g., $\bar{\Lambda}$, might be significantly different from what one expects in pp collisions and give a hint about the properties of the quark-gluon phase.

27.2 Thermodynamics of the Gas Phase and the SBM

Given the grand partition function $Z(\beta, V, \lambda)$ of a many-body system, all thermodynamic quantities can be determined by differentiation of $\ln Z$ with respect to its arguments. Here, λ is the fugacity introduced to conserve a discrete quantum number, here the baryon number. The conservation of strangeness can be carried through in a similar fashion leading then to a further argument λ_s of Z . Whenever necessary, we will consider Z to be implicitly dependent on λ_s .

The grand partition function is a Laplace transform of the level density $\sigma(p, V, b)$, where p_μ is the four-momentum and b the baryon number of the many-body system enclosed in the volume V :

$$Z(\beta, V, \lambda) = \sum_{b=-\infty}^{\infty} \lambda^b \int \sigma(p, V, b) e^{-\beta_\mu p^\mu} d^4 p . \quad (27.2)$$

We recognize the usual relations for the thermodynamic expectation values of the baryon number,

$$\langle b \rangle = \lambda \frac{\partial}{\partial \lambda} \ln Z(\beta, V, \lambda) , \quad (27.3)$$

and the energy–momentum four-vector,

$$\langle p_\mu \rangle = - \frac{\partial}{\partial \beta_\mu} \ln Z(\beta, V, \lambda) , \quad (27.4)$$

which follow from the definition in Eq. (27.2).

The theoretical problem is to determine $\sigma(p, V, b)$ in terms of known quantities. Let us suppose that the physical states of the hadronic gas phase can be considered as being built up from an arbitrary number of massive objects, henceforth called clusters, characterized by a mass spectrum $\tau(m^2, b)$, where $\tau(m^2, b) dm^2$ is the number of different elementary objects (existing in nature) in the mass interval $(m^2, m^2 + dm^2)$ and having the baryon number b . As particle creation must be permitted, the number N of constituents is arbitrary, but constrained by four-momentum conservation and baryon conservation. Neglecting quantum statistics (it can be shown that, for $T \gtrsim 40$ MeV, Boltzmann statistics is sufficient), we have

$$\sigma(p, V, b) = \sum_{N=0}^{\infty} \frac{1}{N!} \int \delta^4 \left(p - \sum_{i=1}^N p_i \right) \sum_{\{b_i\}} \delta_k \left(b - \sum_{i=1}^N b_i \right) \prod_{i=1}^N \frac{2\Delta_\mu p_i^\mu}{(2\pi)^3} \tau(p_i^2, b_i) d^4 p_i . \quad (27.5)$$

The sum over all allowed partitions of b into different b_i is included and Δ is the volume available for the motion of the constituents, which differs from V if the

different clusters carry their proper volume V_{ci} :

$$\Delta^\mu = V^\mu - \sum_{i=1}^N V_{ci}^\mu . \quad (27.6)$$

The phase space volume used in Eq. (27.5) is best explained by considering what happens for one particle of mass m_0 in the rest frame of Δ_μ and β_μ :

$$\int d^4 p_i \frac{2\Delta_\mu p_i^\mu}{(2\pi)^3} e^{-\beta \cdot p} \delta_0(p_i^2 - m^2) = \Delta_0 \int \frac{d^3 p_i}{(2\pi)^3} e^{-\sqrt{p^2 + m^2} \beta_0} = \Delta_0 \frac{Tm^2}{2\pi^2} K_2(m/T) . \quad (27.7)$$

The density of states in Eq. (27.5) implies that the creation and absorption of particles in kinetic and chemical equilibrium is limited only by four-momentum and baryon number conservation. These processes represent the strong hadronic interactions which are dominated by particle productions. $\tau(m^2, b)$ contains all participating elementary particles and their resonances. Some remaining interaction is here neglected or, as we do not use the complete experimental τ , it may be considered as being taken care of by a suitable choice of τ . The short range repulsive forces are taken into account by the introduction of the proper volume V of hadronic clusters.

One more remark concerning the available volume Δ is in order here. If V were considered to be given and an independent thermodynamic quantity, then in Eq. (27.5), a further built-in restriction limits the sum over N to a certain N_{\max} , such that the available volume Δ in Eq. (27.6) remains positive. However, this more conventional assumption of V as the independent variable would significantly obscure our mathematical formalism. It is important to realize that we are *free* to select the available volume Δ as the independent thermodynamic variable and to consider V as a thermodynamic expectation value to be computed from Eq. (27.6):

$$V^\mu \longrightarrow \langle V^\mu \rangle = \Delta^\mu + \langle V_c^\mu(\beta, \Delta, \lambda) \rangle . \quad (27.8)$$

Here $\langle V_c^\mu \rangle$ is the average sum of proper volumes of all hadronic clusters contained in the system considered. As already discussed, the standard quark bag leads to the proportionality between the cluster volume and hadron mass. Similar arguments within the bootstrap model [9, 10], as for example discussed in the preceding Chapter 26 by R. Hagedorn, also lead to

$$\langle V_c^\mu \rangle = \frac{\langle p^\mu(\beta, \Delta, \lambda) \rangle}{4\mathcal{B}} , \quad (27.9)$$

where $4\mathcal{B}$ is the (at this point arbitrary) energy density of isolated hadrons in the quark bag model (for a review, see for example [5]).

Since our hadrons are under pressure from neighbours in hadronic matter, we have in principle to take instead of $4\mathcal{B}$ the energy density of a quark bag exposed to a pressure P [see Eq. (27.57) below]

$$\varepsilon_{\text{bag}} = 4\mathcal{B} + 3P .$$

Combining Eqs. (27.8)–(27.10), we find, with $\varepsilon(\beta, \Delta, \lambda) = \langle p^\mu \rangle / \langle V^\mu \rangle = \langle E \rangle / \langle V \rangle$, that

$$\frac{\Delta}{\langle V(\beta, \Delta, \lambda) \rangle} = 1 - \frac{\varepsilon(\beta, \Delta, \lambda)}{4\mathcal{B} + 3P(\beta, \Delta, \lambda)} . \quad (27.10)$$

As we shall see, the pressure P in the hadronic matter never rises above $\simeq 0.4\mathcal{B}$, see Fig. 27.3a below, and arguments following Eq. (27.63). Consequently, the inclusion of P above—the compression of free hadrons by the hadronic matter by about 10%—may be omitted for now from further discussion. However, we note that both ε and P will be computed as $\ln Z$ becomes available, whence Eq. (27.10) is an implicit equation for $\Delta / \langle V \rangle$.

It is important to record that the expression in Eq. (27.10) can approach zero only when the energy density of the hadronic gas approaches that of matter consisting of one big quark bag: $\varepsilon \rightarrow 4\mathcal{B}$, $P \rightarrow 0$. Thus the density of states in Eq. (27.5), together with the choice of Δ as a thermodynamic variable, is a consistent physical choice only up to this point. Beyond we assume that a description in terms of interacting quarks and gluons is the proper physical description. Bearing all these remarks in mind, we now consider the available volume Δ as a thermodynamic variable which by definition is positive. Inspecting Eq. (27.5) again, we recognize that the level density of the extended objects in volume $\langle V \rangle$ can be interpreted for the time being as the level density of point particles in a fictitious volume Δ :

$$\sigma(p, V, b) = \sigma_{\text{pt}}(p, \Delta, b) , \quad (27.11)$$

whence this is also true for the grand canonical partition function in Eq. (27.2):

$$Z(\beta, V, \lambda) = Z_{\text{pt}}(\beta, \Delta, \lambda) . \quad (27.12)$$

Combining Eqs. (27.2) and (27.5), we also find the important relation

$$\ln Z_{\text{pt}}(\beta, \Delta, \lambda) = \sum_{b=-\infty}^{\infty} \lambda^b \int \frac{2\Delta_\mu p^\mu}{(2\pi)^3} \tau(p^2, b) e^{-\beta_\mu p^\mu} d^4 p . \quad (27.13)$$

This result can only be derived when the sum over N in Eq. (27.5) extends to infinity, thus as long as $\Delta / \langle V \rangle$ in Eq. (27.10) remains positive.

In order to continue with our description of hadronic matter, we must now determine a suitable mass spectrum τ to be inserted into Eq. (27.5). For this we now introduce the statistical bootstrap model. The basic idea is rather old, but has

undergone some development more recently making it clearer, more consistent, and perhaps more convincing. The details may be found in [9] and the references therein. Here a simplified naive presentation is given. We note, however, that our present interpretation is non-trivially different from that in [9].

The basic postulate of statistical bootstrap is that the mass spectrum $\tau(m^2, b)$ containing all the ‘particles’, i.e., elementary, bound states, and resonances (clusters), is generated by the *same* interactions which we see at work if we consider our thermodynamical system. Therefore, if we were to compress this system until it reaches its natural volume $V_c(m, b)$, then it would itself be almost a cluster appearing in the mass spectrum $\tau(m^2, b)$. Since $\sigma(p, \Delta, b)$ and $\tau(p^2, b)$ are both densities of states (with respect to the different parameters d^4p and dm^2), we postulate that

$$\sigma(p, \Delta, b) \Big|_{\substack{(V) \\ \Delta \rightarrow 0}}^{V_c(m, b)} \hat{=} \text{const.} \times \tau(p^2, b), \quad (27.14)$$

where $\hat{=}$ means ‘corresponds to’ (in some way to be specified). As $\sigma(p, \Delta, b)$ is [see Eq. (27.5)] the sum over N of N -fold convolutions of τ , the above ‘bootstrap postulate’ will yield a highly nonlinear integral equation for τ .

The bootstrap postulate (27.14) requires that τ should obey the equation resulting from replacing σ in Eq. (27.5) by some expression containing τ linearly and by taking into account the volume condition expressed in Eqs. (27.8) and (27.9).

We cannot simply put $V = V_c$ and $\Delta = 0$, because now, when each cluster carries its own dynamically determined volume, Δ loses its original meaning and must be redefined more precisely. Therefore, in Eq. (27.5), we tentatively replace

$$\begin{aligned} \sigma(p, V_c, b) &\longrightarrow \frac{2V_c(m, b) \cdot p}{(2\pi)^3} \tau(p^2, b) = \frac{2m^2}{(2\pi)^{34}\mathcal{B}} \tau(p^2, b), \\ \frac{2\Delta \cdot p_i}{(2\pi)^3} \tau(p_i^2, b_i) &\longrightarrow \frac{2V_c(m_i, b_i) \cdot p_i}{(2\pi)^3} \tau(p_i^2, b_i) = \frac{2m_i^2}{(2\pi)^{34}\mathcal{B}} \tau(p_i^2, b_i). \end{aligned} \quad (27.15)$$

Next we argue that the explicit factors m^2 and m_i^2 arise from the dynamics and therefore must be absorbed into $\tau(p_i^2, b_i)$ as dimensionless factors¹ m_i^2/m_0^2 . Thus,

$$\begin{aligned} \sigma(p, V_c, b) &\longrightarrow \frac{2m_0^2}{(2\pi)^{34}\mathcal{B}} \tau(p^2, b) = H\tau(p^2, b), \\ \frac{2\Delta \cdot p_i}{(2\pi)^3} \tau(p_i^2, b_i) &\longrightarrow \frac{2m_0^2}{(2\pi)^{34}\mathcal{B}} \tau(p_i^2, b_i) = H\tau(p_i^2, b_i), \end{aligned} \quad (27.16)$$

¹Here is the essential difference with [9], where another choice was made.

with

$$H = \frac{2m_0^2}{(2\pi)^3 4\mathcal{B}},$$

where either H or m_0 may be taken as a new free parameter of the model, to be fixed later. (If m_0 is taken, then it should be of the order of the ‘elementary masses’ appearing in the system, e.g., somewhere between m_π and M_N in a model using pions and nucleons as elementary input.) Finally, if clusters consist of clusters which consist of clusters, and so on, this should end at some ‘elementary’ particles (where what we consider as elementary is fixed by convention). Inserting Eq. (27.16) into Eq. (27.5), the bootstrap equation (BE) then reads

$$H\tau(p^2, b) = Hg_b\delta_0(p^2 - \bar{m}_b^2) \quad (27.17)$$

$$+ \sum_{N=2}^{\infty} \frac{1}{N!} \int \delta^4\left(p - \sum_{i=1}^N p_i\right) \sum_{\{b_i\}} \delta_k\left(b - \sum_{i=1}^N b_i\right) \prod_{i=1}^N H\tau(p_i^2, b_i) d^4 p_i.$$

Clearly, the bootstrap equation (27.17) has not been derived. We have made it more or less plausible and state it as a postulate. For more motivation, see [9]. In other words, the bootstrap equation means that the cluster with mass $\sqrt{p^2}$ and baryon number b is either elementary (mass \bar{m}_b , spin isospin multiplicity g_b), or it is composed of any number $N \geq 2$ of subclusters having the same internal composite structure described by this equation. The bar over \bar{m}_b indicates that one has to take the mass which the ‘elementary particle’ will have effectively when present in a large cluster, e.g., in nuclear matter, $\bar{m} = m - \langle E_{\text{bind}} \rangle$, and $\bar{m}_N \approx 925$ MeV. That this must be so becomes obvious if one imagines Eq. (27.17) solved by iteration (the iteration solution exists and is the physical solution). Then $H\tau(p^2, b)$ becomes in the end a complicated function of p^2 , b , all \bar{m}_b , and all g_b . In other words, in the end a single cluster consists of the ‘elementary particles’. As these are all bound into the cluster, their mass \bar{m} should be the effective mass, not the free mass m . This way we may include a small correction for the long-range attractive meson exchange by choosing $\bar{m}_N = m - 15$ MeV.

Let us make a brief excursion to the bag model at this point. There the mass of a hadron is computed from the assumption of an *isolated* particle (= bag) with its size and mass being determined from the equilibrium between the vacuum pressure \mathcal{B} and the internal Fermi pressure of the (valence) quarks. In a hadron gas, this is not true as a finite pressure is exerted on hadrons in matter. After a short calculation, we find the pressure dependence of the bag model hadronic mass:

$$M(P) = M(0) \frac{1 + 3P/4\mathcal{B}}{(1 + P/\mathcal{B})^{3/4}} = M(0) \left[1 + \frac{3}{32} \left(\frac{P}{\mathcal{B}} \right)^2 + \dots \right]. \quad (27.18)$$

We have already noted that the pressure never exceeds $0.4\mathcal{B}$ in the hadronic gas phase, see Fig. 27.3a below, and arguments following Eq. (27.63). Hence we see that the increase in mass of constituents (quark bags) in the hadronic gas never exceeds 1.5% and is at most comparable with the 15 MeV binding in \bar{m} . In general, P is about $0.1B$ and the pressure effect may be neglected.

Thus we can consider the ‘input’ first term in Eq. (27.17) as being fixed by pions, nucleons, and whenever necessary by the usual strange members of meson and baryon multiplets. Furthermore, we note that the bootstrap equation (27.17) makes use of practically all the same approximations as our description of the level density in Eq. (27.5). Thus the solution of Eq. (27.17) is particularly suitable for our use.

We solve the BE by the same double Laplace transformation which we used before Eq. (27.2). We define

$$\begin{aligned}\varphi(\beta, \lambda) &:= \int e^{-\beta_\mu p^\mu} \sum_{b=-\infty}^{\infty} \lambda^b H g_b \delta_0(p^2 - \bar{m}_b^2) d^4 p = 2\pi HT \sum_{b=-\infty}^{\infty} \lambda^b g_b \bar{m}_b K_1(\bar{m}_b/T), \\ \Phi(\beta, \lambda) &:= \int e^{-\beta_\mu p^\mu} \sum_{b=-\infty}^{\infty} \lambda^b H \tau(p^2, b) d^4 p.\end{aligned}\quad (27.19)$$

Once the set of input particles $\{\bar{m}_b, g_b\}$ is given, $\varphi(\beta, \lambda)$ is a known function, while $\Phi(\beta, \lambda)$ is unknown. Applying the double Laplace transformation to the BE, we obtain

$$\Phi(\beta, \lambda) = \varphi(\beta, \lambda) + \exp \Phi(\beta, \lambda) - \Phi(\beta, \lambda) - 1. \quad (27.20)$$

This implicit equation for Φ in terms of φ can be solved without regard for the actual β, λ dependence. Writing

$$G(\varphi) := \Phi(\beta, \lambda), \quad \varphi = 2G - e^G + 1, \quad (27.21)$$

we can draw the curve $\varphi(G)$, see Fig. 17.5a, and then invert it graphically, see Fig. 17.5b to obtain $G(\varphi) = \Phi(\beta, \lambda)$. $G(\varphi)$ has a square root singularity at $\varphi = \varphi_0 = \ln(4/e) = 0.3863$. Beyond this value, $G(\varphi)$ becomes complex. There are further branches; for example Fig. 17.5b the *dashed line* represents the unphysical real solution branch.

Apart from this graphical solution, other forms of solution are known:

$$G(\varphi) = \sum_{n=1}^{\infty} s_n \varphi^n = \sum_{n=0}^{\infty} w_n (\varphi_0 - \varphi)^{n/2} = \text{integral representation}. \quad (27.22)$$

The expansion in terms of $(\varphi_0 - \varphi)^{n/2}$ has been used in our numerical work (12 terms yield a solution within computer accuracy) and the integral representation will be published elsewhere [15]. Henceforth, we consider $\Phi(\beta, \lambda) = G(\varphi)$ to be

a known function of $\varphi(\beta, \lambda)$. Consequently, $\tau(m^2, b)$ is also in principle known. From the singularity at $\varphi = \varphi_0$, it follows [1] that $\tau(m^2, b)$ grows, for $m \gg m_N b$, exponentially $\sim m^{-3} \exp(m/T_0)$. In some weaker form, this has been known for a long time [7, 16, 17].

27.3 The Hot Hadronic Gas

The definition of $\Phi(\beta, \lambda)$ in Eq. (27.19) in terms of the mass spectrum allows us to write a very simple expression for $\ln Z$ in the gas phase (passing now to the rest frame of the gas):

$$\ln Z(\beta, V, \lambda) = \ln Z_{\text{pt}}(\beta, \Delta, \lambda) = -\frac{2\Delta}{(2\pi)^3 H} \frac{\partial}{\partial \beta} \Phi(\beta, \lambda). \quad (27.23)$$

We recall that Eqs. (27.10) and (27.20) define (implicitly) the quantities Δ and Φ in terms of the physical variables V , β , and λ .

Let us now introduce the energy density ε_{pt} of the hypothetical pointlike particles as

$$\varepsilon_{\text{pt}}(\beta, \lambda) = \frac{1}{\Delta} \left[-\frac{\partial}{\partial \beta} \ln Z_{\text{pt}}(\beta, \Delta, \lambda) \right] = \frac{2}{(2\pi)^3 H} \frac{\partial^2}{\partial \beta^2} \Phi(\beta, \lambda), \quad (27.24)$$

which will turn out to be quite helpful as it is independent of Δ . The proper energy density is

$$\varepsilon(\beta, \lambda) = \frac{1}{\langle V \rangle} \left(-\frac{\partial}{\partial \beta} \ln Z \right) = \frac{\Delta}{\langle V \rangle} \varepsilon_{\text{pt}}, \quad (27.25)$$

while the pressure follows from

$$P(\beta, \lambda) \langle V \rangle = T \ln Z(\beta, V, \lambda) = T \ln Z_{\text{pt}}(\beta, \Delta, \lambda), \quad (27.26)$$

$$P(\beta, \lambda) = \frac{\Delta}{\langle V \rangle} \left[-\frac{2T}{(2\pi)^3 H} \frac{\partial}{\partial \beta} \Phi(\beta, \lambda) \right] =: \frac{\Delta}{\langle V \rangle} P_{\text{pt}}. \quad (27.27)$$

Similarly, for the baryon number density, we find

$$\nu(\beta, \lambda) = \frac{\langle b \rangle}{\langle V \rangle} =: \frac{\Delta}{\langle V \rangle} \nu_{\text{pt}}(\beta, \lambda), \quad (27.28)$$

with

$$\nu_{\text{pt}}(\beta, \lambda) = \frac{1}{\Delta} \lambda \frac{\partial}{\partial \lambda} \ln Z_{\text{pt}} = -\frac{2}{(2\pi)^3 H} \lambda \frac{\partial}{\partial \lambda} \frac{\partial}{\partial \beta} \Phi(\beta, \lambda). \quad (27.29)$$

From Eqs. (27.24)–(27.24), the crucial role played by the factor $\Delta/\langle V \rangle$ becomes apparent. We note that it is quite straightforward to insert Eqs. (27.25) and (27.26) into Eq. (27.10) and solve the resulting quadratic equation to obtain $\Delta/\langle V \rangle$ as an explicit function of ε_{pt} and P_{pt} . First we record the limit $P \ll B$:

$$\frac{\Delta}{\langle V \rangle} = 1 - \frac{\varepsilon(\beta, \lambda)}{4\mathcal{B}} = \left[1 + \frac{\varepsilon_{\text{pt}}(\beta, \lambda)}{4\mathcal{B}} \right]^{-1}, \quad (27.30)$$

while the correct expression is

$$\frac{\Delta}{\langle V \rangle} = \frac{1}{2} - \frac{\varepsilon_{\text{pt}}}{6P_{\text{pt}}} - \frac{2\mathcal{B}}{3P_{\text{pt}}} + \sqrt{\frac{4\mathcal{B}}{3P_{\text{pt}}} + \left(\frac{1}{2} - \frac{\varepsilon_{\text{pt}}}{6P_{\text{pt}}} - \frac{2\mathcal{B}}{3P_{\text{pt}}} \right)^2}. \quad (27.31)$$

The last of the important thermodynamic quantities is the entropy S . By differentiating Eq. (27.26), we find

$$\frac{\partial}{\partial \beta} \ln Z = \frac{\partial}{\partial \beta} \beta P \langle V \rangle = P \langle V \rangle - T \frac{\partial}{\partial T} (P \langle V \rangle). \quad (27.32)$$

Considering Z as a function of the chemical potential, viz.,

$$Z(\beta, V, \lambda) = Z(\beta, V, e^{\mu\beta}) = \tilde{Z}(\beta, V, \mu) = \tilde{Z}_{\text{pt}}(\beta, \Delta, \mu), \quad (27.33)$$

we find

$$\frac{\partial}{\partial \beta} \ln Z \Big|_{\mu, \Delta} = \frac{\partial}{\partial \beta} \ln \tilde{Z}_{\text{pt}}(\beta, \Delta, \mu) = -E + \mu \langle b \rangle, \quad (27.34)$$

with E being the total energy. From Eqs. (27.32) and (27.34), we find the ‘first law’ of thermodynamics to be

$$E = -P \langle V \rangle + T \frac{\partial}{\partial T} (P \langle V \rangle) + \mu \langle b \rangle. \quad (27.35)$$

Now quite generally,

$$E = -P \langle V \rangle + TS + \mu \langle b \rangle, \quad (27.36)$$

so that

$$S = \frac{\partial}{\partial T} \left[P(\beta, \Delta, \mu) \langle V(\beta, \Delta, \mu) \rangle \right] \Big|_{\mu, \Delta}. \quad (27.37)$$

Equations (27.26) and (27.34) now allow us to write

$$S = \frac{\partial}{\partial T}(P\langle V \rangle) = \ln \tilde{Z}_{\text{pt}}(T, \Delta, \mu) + \frac{E - \mu b}{T} . \quad (27.38)$$

The entropy density in terms of the already defined quantities is therefore

$$\mathcal{S} = \frac{S}{\langle V \rangle} = \frac{P + \varepsilon - \mu\nu}{T} . \quad (27.39)$$

We shall now take a brief look at the quantities P , ε , ν , $\Delta/\langle V \rangle$. They can be written in terms of $\partial\Phi(\beta, \lambda)/\partial\beta$ and its derivatives. We note that [see Eq. (27.21)]

$$\frac{\partial}{\partial\beta}\Phi(\beta, \lambda) = \frac{\partial G(\varphi)}{\partial\varphi} \frac{\partial\varphi}{\partial\beta} , \quad (27.40)$$

and that $\partial G/\partial\varphi \sim (\varphi_0 - \varphi)^{-1/2}$ near to $\varphi = \varphi_0 = \ln(4/e)$ (see Fig. 17.5b). Hence at $\varphi = \varphi_0$, we find a singularity in the point particle quantities ε_{pt} , ν_{pt} , and P_{pt} . This implies that all hadrons have coalesced into one large cluster. Indeed, from Eqs. (27.25), (27.27), (27.28), and (27.30), we find

$$\begin{aligned} \varepsilon &\longrightarrow 4\mathcal{B} , \\ P &\longrightarrow 0 , \\ \Delta/\langle V \rangle &\longrightarrow 0 . \end{aligned} \quad (27.41)$$

We can easily verify that this is correct by establishing the average number of clusters present in the hadronic gas. This is done by introducing an artificial fugacity ξ^N in Eq. (27.5) in the sum over N , where N is the number of clusters. Denoting by $Z(\xi)$ the associated grand canonical partition functions in Eq. (27.23), we find

$$\langle N \rangle = \xi \frac{\partial}{\partial\xi} \ln Z_{\text{pt}}^{\xi}(\beta, \Delta, \lambda; \xi) \Big|_{\xi=1} = -\frac{2\Delta}{(2\pi)^3 H} \frac{\partial}{\partial\beta} \Phi(\beta, \lambda) , \quad (27.42)$$

which leads to the useful relation

$$P\langle V \rangle = \langle N \rangle T . \quad (27.43)$$

Thus as $P\langle V \rangle \rightarrow 0$, so must $\langle N \rangle$, the number of clusters, for finite T . We record the astonishing fact that the hadron gas phase obeys an ‘ideal’ gas equation, although of course $\langle N \rangle$ is not constant as for a real ideal gas but a function of the thermodynamic variables.

The boundary given by

$$\varphi(\beta, \lambda) = \varphi_0 = \ln(4/e) \quad (27.44)$$

thus defines a critical curve in the β, λ plane. Its position depends, of course, on the actually given form of $\varphi(\beta, \lambda)$, i.e., on the set of ‘input’ particles $\{\bar{m}_b, g_b\}$ assumed and the value of the constant H in Eq. (27.16). In the case of three elementary pions π^+, π^0 , and π^- and four elementary nucleons (spin \otimes isospin) and four antinucleons, we have from Eq. (27.19)

$$\varphi(\beta, \lambda) = 2\pi HT \left[3m_\pi K_1(m_\pi/T) + 4 \left(\lambda + \frac{1}{\lambda} \right) \bar{m}_N K_1(\bar{m}_N/T) \right], \quad (27.45)$$

and the condition (27.44), written in terms of T and $\mu = T \ln \lambda$, yields the curve shown in Fig. 25.3 i.e., the ‘critical curve’, corresponding to $\varphi(T, \mu) = \varphi_0$ in the μ, T plane. Beyond it, the usual hadronic world ceases to exist. In the shaded region our theory is not valid, because we neglected Bose-Einstein and Fermi-Dirac statistics. For $\mu = 0$, the curve ends at $T = T_0$, where T_0 , the ‘limiting temperature of hadronic matter’, is the same as that appearing in the mass spectrum [7, 9, 16, 17] $\tau(m^2, b) \sim m^{-3} \exp(m/T_0)$ (for $b \gg bm_N$).

The value of the constant H in Eq. (27.16) has been chosen [13] to yield $T_0 = 190 \text{ MeV}$. This apparently large value of T_0 seemed necessary to yield a maximal average decay temperature of the order of 145 MeV , as required by [18]. (However, a new value of the bag constant then induces a change [1] to a lower value of $T_0 = 180 \text{ MeV}$.) Here we use

$$\begin{aligned} H &= 0.724 \text{ GeV}^{-2}, & T_0 &= 0.19 \text{ GeV}, \\ m_0 &= 0.398 \text{ GeV} \quad [\text{when } \mathcal{B} = (145 \text{ MeV})^4], \end{aligned} \quad (27.46)$$

where the value of m_0 lies as expected between m_π and m_N [$(m_\pi m_N)^{1/2} = 0.36 \text{ GeV}$].

The critical curve limits the hadron gas phase. By approaching it, all hadrons dissolve into a giant cluster, which is not in our opinion a hadron solid [14]. We would prefer to identify it with a quark-gluon plasma. Indeed, as the energy density along the critical curve is constant ($= 4\mathcal{B}$), the critical curve can be attained and, if the energy density becomes $> 4\mathcal{B}$, we enter into a region which cannot be described without making assumptions about the inner structure and dynamics of the ‘elementary particles’ $\{\bar{m}_b, g_b\}$ —here pions and nucleons—entering into the input function $\varphi(\beta, \lambda)$. Considering pions and nucleons as quark-gluon bags leads naturally to this interpretation.

27.4 The Quark–Gluon Phase

We now turn to the discussion of the region of the strongly interacting matter in which the energy density would be equal to or higher than $4\mathcal{B}$. As a basic postulate, we will assume that it consists of—relatively weakly—interacting quarks. To begin with, only u and d flavours will be considered as they can easily be copiously

produced at $T \gtrsim 50 \text{ MeV}$. Again the aim is to derive the grand partition function Z . This is a standard exercise. For the massless quark Fermi gas up to first order in the interaction [1, 2, 12], the result is

$$\ln Z_q(\beta, \lambda) = \frac{8V}{6\pi^2} \beta^{-3} \left[\left(1 - \frac{2\alpha_s}{\pi}\right) \left(\frac{1}{4} \ln^4 \lambda_q + \frac{\pi^2}{2} \ln^2 \lambda_q\right) + \left(1 - \frac{50\alpha_s}{21\pi}\right) \frac{7\pi^4}{60} \right], \quad (27.47)$$

valid in the limit $m_q < T \ln \lambda_q$.

Here $g = (2s + 1)(2I + 1)C = 12$ counts the number of the components of the quark gas, and λ_q is the fugacity related to the quark number. As each quark has baryon number $1/3$, we find

$$\lambda_q^3 = \lambda = e^{\mu/T}, \quad (27.48)$$

where as before λ allows for conservation of the baryon number. Consequently,

$$3\mu_q = \mu. \quad (27.49)$$

The glue contribution is

$$\ln Z_g(\beta, \lambda) = V \frac{8\pi^2}{45} \beta^{-3} \left(1 - \frac{15\alpha_s}{4\pi}\right). \quad (27.50)$$

We notice the two relevant differences with the photon gas:

- The occurrence of the factor eight associated with the number of gluons.
- The glue–glue interaction as gluons carry colour charge.

Finally, let us introduce the vacuum term, which accounts for the fact that the perturbative vacuum is an excited state of the ‘true’ vacuum which has been renormalized to have a vanishing thermodynamic potential, $\Omega = -\beta^{-1} \ln Z$. Hence in the perturbative vacuum,

$$\ln Z_{\text{vac}} = -\beta \mathcal{B}V. \quad (27.51)$$

This leads to the required positive energy density \mathcal{B} within the volume occupied by the coloured quarks and gluons and to a negative pressure on the surface of this region. At this stage, this term is entirely phenomenological, as discussed above. The equations of state for the quark–gluon plasma are easily obtained by differentiating

$$\ln Z = \ln Z_q + \ln Z_g + \ln Z_{\text{vac}} \quad (27.52)$$

with respect to β , λ , and V . The baryon number density, energy, and pressure are respectively:

$$\nu = \frac{1}{V} \lambda \frac{\partial}{\partial \lambda} \ln Z = \frac{2T^3}{\pi^2} \left(1 - \frac{2\alpha_s}{\pi}\right) \left(\frac{1}{3^4} \ln^3 \lambda + \frac{\pi^2}{9} \ln \lambda\right), \quad (27.53)$$

$$\begin{aligned} \varepsilon &= -\frac{1}{V} \frac{\partial}{\partial \beta} \ln Z \\ &= \frac{6}{\pi^2} T^4 \left[\left(1 - \frac{2\alpha_s}{\pi}\right) \left(\frac{1}{4 \cdot 3^4} \ln^4 \lambda + \frac{\pi^2}{2 \cdot 3^2} \ln^2 \lambda\right) + \left(1 - \frac{50\alpha_s}{21\pi}\right) \frac{7\pi^4}{60} \right] \\ &\quad + \frac{8\pi^2}{15} T^4 \left(1 - \frac{15\alpha_s}{4\pi}\right) + \mathcal{B}, \end{aligned} \quad (27.54)$$

$$\begin{aligned} P &= T \frac{\partial}{\partial V} \ln Z \\ &= \frac{2T^4}{\pi^2} \left[\left(1 - \frac{2\alpha_s}{\pi}\right) \left(\frac{1}{4 \cdot 3^4} \ln^4 \lambda + \frac{\pi^2}{2 \cdot 3^2} \ln^2 \lambda\right) + \left(1 - \frac{50\alpha_s}{21\pi}\right) \frac{7\pi^4}{60} \right] \\ &\quad + \frac{8\pi^2}{45} T^4 \left(1 - \frac{15\alpha_s}{4\pi}\right) - \mathcal{B}. \end{aligned} \quad (27.55)$$

Let us first note that, for $T \ll \mu$ and $P = 0$, the baryon chemical potential tends to

$$\mu_B = 3\mu_q \longrightarrow 3\mathcal{B}^{1/4} \left[\frac{2\pi^2}{(1 - 2\alpha_s/\pi)} \right]^{1/4} = 1010 \text{ MeV}, \quad \alpha_s = 1/2, \quad \mathcal{B}^{1/4} = 145 \text{ MeV}, \quad (27.56)$$

which assures us that interacting cold quark matter is an excited state of nuclear matter. We have assumed that, except for T , there is no relevant dimensional parameter, e.g., quark mass m_q or the quantity Λ which enters into the running coupling constant $\alpha_s(q^2)$. Therefore the relativistic relation between the energy density and pressure, viz., $\varepsilon - \mathcal{B} = 3(P + \mathcal{B})$, is preserved, which leads to

$$P = \frac{1}{3}(\varepsilon - 4\mathcal{B}), \quad (27.57)$$

a relation we have used occasionally before [see Eq. (27.10)].

From Eq. (27.57), it follows that, when the pressure vanishes, the energy density is $4\mathcal{B}$, independent of the values of μ and T which fix the line $P = 0$. This behaviour is consistent with the hadronic gas phase. This may be used as a reason to choose the parameters of both phases in such a way that the two lines $P = 0$ coincide. We

will return to this point again below. For $P > 0$, we have $\varepsilon > 4\mathcal{B}$. Recall that, in the hadronic gas, we had $0 < \varepsilon < 4\mathcal{B}$. Thus, above the critical curve of the μ, T plane, we have the quark-gluon plasma exposed to an external force.

In order to obtain an idea of the form of the $P = 0$ critical curve in the μ, T plane for the quark-gluon plasma, we rewrite Eq. (27.55) using Eqs. (27.48) and (27.49) for $P = 0$:

$$\mathcal{B} = \frac{1 - 2\alpha_s/\pi}{162\pi^2} [\mu^2 + (3\pi T)^2]^2 + \frac{T^4 \pi^2}{45} \left[12 \left(1 - \frac{5\alpha_s}{3\pi} \right) + 8 \left(1 - \frac{15\alpha_s}{4\pi} \right) \right]. \quad (27.58)$$

Here, the last term is the glue pressure contribution. (If the true vacuum structure is determined by the glue–glue interaction, then this term could be modified significantly.) We find that the greatest lower bound on temperature T_q at $\mu = 0$ is about

$$T_q \sim \mathcal{B}^{1/4} \approx 145\text{--}190 \text{ MeV}. \quad (27.59)$$

This result can be considered to be correct to within 20%. Its order of magnitude is as expected. Taking Eq. (27.58) as it is, we find for $\alpha_s = 1/2$, $T_q = 0.88\mathcal{B}^{1/4}$. Omitting the gluon contribution to the pressure, we find $T_q = 0.9\mathcal{B}^{1/4}$. It is quite likely that, with the proper treatment of the glue field and the plasma corrections, and with larger $\mathcal{B}^{1/4} \sim 190 \text{ MeV}$, the desired value of $T_q = T_0$ corresponding to the statistical bootstrap choice will follow. Furthermore, allowing some reasonable T, μ dependence of α_s , we can then easily obtain an agreement between the critical curves.

However, it is not necessary for the two critical curves to coincide, even though this would be preferable. As the quark plasma is the phase into which individual hadrons dissolve, it is sufficient if the quark plasma pressure vanishes within the boundary set for non-vanishing positive pressure of the hadronic gas. It is quite satisfactory for the theoretical development that this is the case. In Fig. 27.1a, a qualitative picture of the two $P = 0$ lines is shown in the μ, T plane. Along the dotted straight line at constant temperature, we show in Fig. 27.1b the pressure as a function of the volume (a P, V diagram). The volume is obtained by inverting the baryon density at constant fixed baryon number:

$$V = \frac{\langle b \rangle}{\nu}. \quad (27.60)$$

The behaviour of $P(V, T = \text{const.})$ for the hadronic gas phase is as described before in the statistical bootstrap model. For large volumes, we see that P falls with rising V . However, when hadrons get close to each other so that they form larger and larger lumps, the pressure drops rapidly to zero. The hadronic gas becomes a state of few composite clusters (internally already consisting of the quark plasma). The second branch of the $P(V, T = \text{const.})$ line meets the first one at a certain volume $V = V_m$.

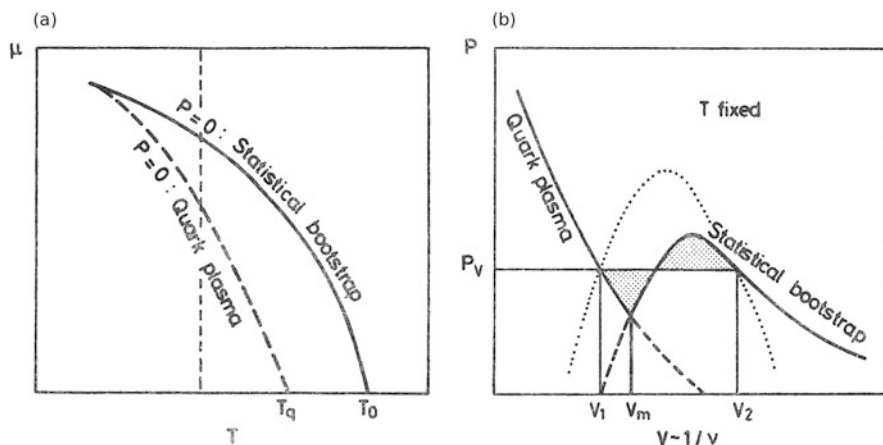


Fig. 27.1 (a) The critical curves ($P = 0$) of the two models in the T, μ plane (qualitatively). The region below the *full line* is described by the statistical bootstrap model and the region above the *broken line* by the quark-gluon plasma. The critical curves can be made to coincide. (b) P, V diagram (qualitative) of the phase transition (hadron gas to quark-gluon plasma) along the *broken line* $T = \text{const.}$ of (a). The coexistence region is found from the usual Maxwell construction (the *shaded areas* being equal)

The phase transition occurs for $T = \text{const.}$ in Fig. 27.1b at a vapour pressure P_V obtained from the conventional Maxwell construction: the shaded regions in Fig. 27.1b are equal. Between the volumes V_1 and V_2 , matter coexists in the two phases with the relative fractions being determined by the magnitude of the actual volume. This leads to the occurrence of a third region, viz., the coexistence region of matter, in addition to the pure quark and hadron domains. For $V < V_1$, corresponding to $v > v_1 \sim 1/V_1$, all matter has gone into the quark plasma phase.

The dotted line in Fig. 27.1b encloses (qualitatively) the domain in which the coexistence between the two phases of hadronic matter seems possible. We further note that, at low temperatures $T \leq 50 \text{ MeV}$, the plasma and hadronic gas critical curves meet each other in Fig. 27.1a. This is just the domain where, at present, our description of the hadronic gas fails, while the quark-gluon plasma also begins to suffer from infrared difficulties. Both approaches have a very limited validity in this domain.

The qualitative discussion presented above can be easily supplemented with quantitative results. But first we turn our attention to the modifications forced onto this simple picture by the experimental circumstances in high energy nuclear collisions.

27.5 Nuclear Collisions and Inclusive Particle Spectra

We assume that in relativistic collisions triggered to small impact parameters by high multiplicities and absence of projectile fragments [19], a hot central fireball of hadronic matter can be produced. We are aware of the whole problematic connected with such an idealization. A proper treatment should include collective motions and distribution of collective velocities, local temperatures, and so on [20], as explained in the preceding Chapter 26 by R. Hagedorn [10]. Triggering for high multiplicities hopefully eliminates some of the complications. In nearly symmetric collisions (projectile and target nuclei are similar), we can argue that the numbers of participants in the centre of mass of the fireball originating in the projectile or target are the same. Therefore, it is irrelevant how many nucleons do form the fireball—and the above symmetry argument leads, in a straightforward way, to a formula for the centre of mass energy per participating nucleon:

$$U := \frac{E_{\text{c.m.}}}{A} = m_N \sqrt{1 + \frac{E_{\text{k,lab}}/A}{2m_N}}, \quad (27.61)$$

where $E_{\text{k,lab}}/A$ is the projectile kinetic energy per nucleon in the laboratory frame. While the fireball changes its baryon density and chemical composition ($\pi + p \leftrightarrow \Delta$, etc.) during its lifetime through a change in temperature and chemical potential, the conservation of energy and baryon number assures us that U in Eq. (27.61) remains constant, assuming that the influence on U of pre-equilibrium emission of hadrons from the fireball is negligible. As U is the total energy per baryon available, we can, supposing that kinetic and chemical equilibrium have been reached, set it equal to the ratio of thermodynamic expectation values of the total energy and baryon number:

$$U = \frac{\langle E \rangle}{\langle b \rangle} = \frac{E(\beta, \lambda)}{\nu(\beta, \lambda)}. \quad (27.62)$$

Thus we see that, through Eq. (27.62), the experimental value of U in Eq. (27.61) fixes a relation between allowable values of β, λ : the available excitation energy defines the temperature and the chemical composition of hadronic fireballs. In Fig. 27.2a, b, these paths are shown for a choice of kinetic energies $E_{\text{k,lab}}/A$ in the μ, T plane and in the ν, T plane, respectively. In both cases, only the hadronic gas domain is shown. We wish to note several features of the curves shown in Fig. 27.2 that will be relevant in later considerations:

1. Beginning at the critical curve, the chemical potential first drops rapidly when T decreases and then rises slowly as T decreases further (Fig. 27.2a). This corresponds to a monotonically falling baryon density with decreasing temperature (Fig. 27.2b), but implies that, in the initial expansion phase of the fireball, the chemical composition changes more rapidly than the temperature.

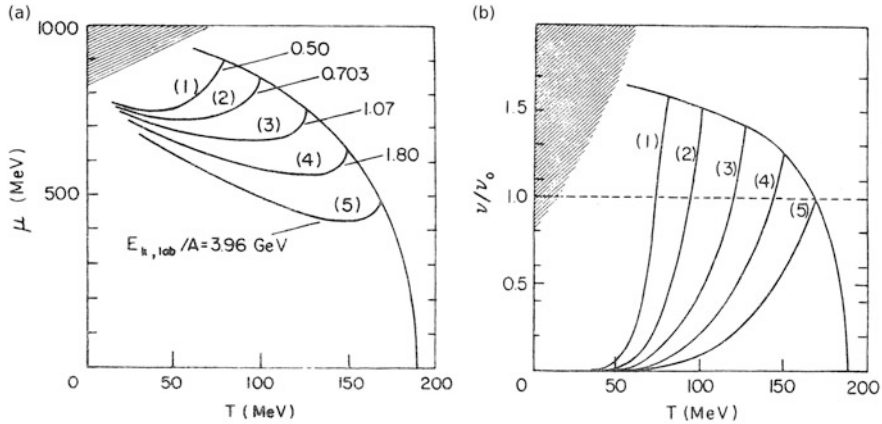


Fig. 27.2 (a) The critical curve of hadron matter (bootstrap), together with some ‘cooling curves’ in the T, μ plane. While the system cools down along these lines, it emits particles. When all particles have become free, it comes to rest on some point on these curves (‘freeze out’). In the *shaded region*, our approach may be invalid. (b) The critical curve of hadron matter (bootstrap), together with some ‘cooling curves’ [same energy as in (a)] in the variables T and $\nu/\nu_0 =$ ratio of baryon number density to normal nuclear baryon number density. In the *shaded region*, our approach may be invalid

2. The baryon density in Fig. 27.2b is of the order of 1–1.5 of normal nuclear density. This is a consequence of the choice of $\mathcal{B}^{1/4} = 145 \text{ MeV}$. Were \mathcal{B} three times as large, i.e., $\mathcal{B}^{1/4} = 190 \text{ MeV}$, which is so far not excluded, then the baryon densities in this figure would triple to $3\text{--}5\nu_0$. Furthermore, we observe that, along the critical curve of the hadronic gas, the baryon density falls with rising temperature. This is easily understood as, at higher temperature, more volume is taken up by the numerous mesons.
3. Inspecting Fig. 27.2b, we see that, at given U , the temperatures at the critical curve and those at about $\nu_0/2$ differ little (10%) for low U , but more significantly for large U . Thus, highly excited fireballs cool down more before dissociation (‘freeze out’). As particles are emitted all the time while the fireball cools down along the lines of Fig. 27.2, they carry kinetic energies related to various different temperatures. The inclusive single particle momentum distribution will yield only averages along these cooling lines.

Another remark which does not follow from the curves shown is:

4. Below about 1.8 GeV, an important portion of the total energy is in the collective (hydrodynamical) motion of hadronic matter, whence the cooling curves at constant excitation energy do not properly describe the evolution of the fireball.

Calculations of this kind can also be carried out for the quark plasma. They are, at present, uncertain due to the unknown values of α_s and $\mathcal{B}^{1/4}$. Fortunately, there is one particular property of the equation of state of the quark-gluon plasma that we

can easily exploit. Combining Eq. (27.57) with Eq. (27.62), we obtain

$$P = \frac{1}{3}(U\nu - 4\mathcal{B}) . \tag{27.63}$$

Thus, for a given U (the available energy per baryon in a heavy ion collision), Eq. (27.63) describes the pressure–volume ($\sim 1/\nu$) relation. By choosing to measure P in units of \mathcal{B} and ν in units of normal nuclear density $\nu_0 = 0.14/\text{fm}^3$, we find

$$\frac{P}{\mathcal{B}} = \frac{4}{3} \left(\gamma \frac{U}{m_N} \frac{\nu}{\nu_0} - 1 \right) , \tag{27.64}$$

with

$$\gamma := \frac{m_N \nu_0}{4\mathcal{B}} = 0.56 , \quad \mathcal{B}^{1/4} = 145 \text{ MeV} , \quad \nu_0 = 0.14/\text{fm}^3 .$$

Here, γ is the ratio of the energy density of normal nuclei ($\varepsilon_N = m_N \nu_0$) and of quark matter or of a quark bag ($\varepsilon_q = 4\mathcal{B}$). In Fig. 27.3a, this relation is shown for three projectile energies: $E_{k,\text{lab}}/A = 1.80 \text{ GeV}$, 3.965 GeV , and 5.914 GeV , corresponding to $U = 1.314 \text{ GeV}$, 1.656 GeV , and 1.913 GeV , respectively. We observe that, even at the lowest energy shown, the quark pressure is zero near the baryon density corresponding to 1.3 normal nuclear density, given the current value of \mathcal{B} .

Before discussing this point further, we note that the hadronic gas branches of the curves in Fig. 27.3 show a quite similar behaviour to that shown at constant temperature in Fig. 27.1b. Remarkably enough, the two branches meet each other

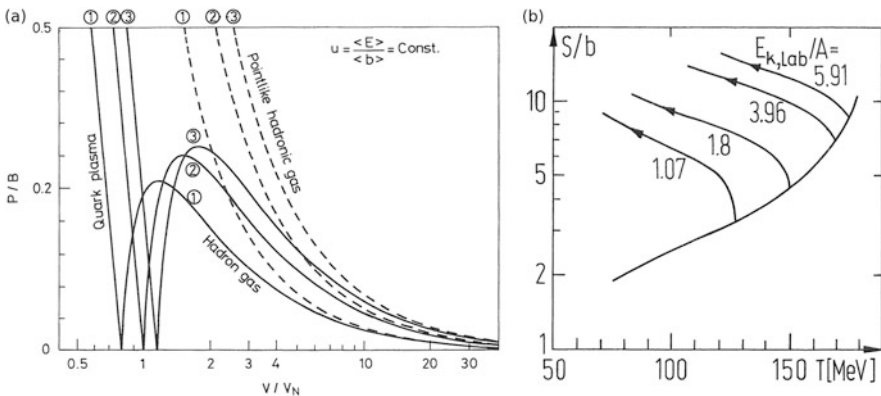


Fig. 27.3 (a) P, V diagram of ‘cooling curves’ belonging to different kinetic laboratory energies per nucleon: (1) 1.8 GeV, (2) 3.965 GeV, (3) 5.914 GeV. In the history of a collision, the system comes down the quark lines and jumps somewhere over to the hadron curves (Maxwell). *Broken lines* show the diverging pressure of pointlike bootstrap hadrons. (b) The total specific entropy per baryon in the hadronic gas phase. Same energies per nucleon as in (a) and a fourth value 1.07 GeV

at $P = 0$, since both have the same energy density $\varepsilon = 4\mathcal{B}$ and therefore $V(P = 0) \sim 1/\nu = U/\varepsilon = U/4\mathcal{B}$. However, what we cannot see by inspecting Fig. 27.3 is that there will be a discontinuity in the variables μ and T at this point, except if parameters are chosen so that the critical curves of the two phases coincide. Indeed, near to $P = 0$, the results shown in Fig. 27.3a should be replaced by points obtained from the Maxwell construction. The pressure in a nuclear collision will never fall to zero. It will correspond to the momentary vapour pressure of the order of $0.2\mathcal{B}$ as the phase change occurs.

A further aspect of the equations of state for the hadronic gas is also illustrated in Fig. 27.3a. Had we ignored the finite size of hadrons (one of the van der Waals effects) in the hadron gas phase then, as shown by the dash-dotted lines, the phase change could never occur because the point particle pressure would diverge where the quark pressure vanishes. In our opinion, one cannot say it often enough: inclusion of the finite hadronic size and of the finite temperature when considering the phase transition to quark plasma lowers the relevant baryon density (from 8–14 ν_0 for cold point-nucleon matter) to 1–5 ν_0 (depending on the choice of \mathcal{B}) in 2–5 GeV/A nuclear collisions [21].

The physical picture underlying our discussion is an explosion of the fireball into vacuum with little energy being converted into collective motion, e.g., hydrodynamical flow, or being taken away by fast pre-hadronization particle emission. Thus the conserved internal excitation energy can only be shifted between thermal (kinetic) and chemical excitations of matter. ‘Cooling’ thus really means that, during the explosion, the thermal energy is mostly converted into chemical energy, e.g., *pions are produced*.

While it is at present hard to judge the precise amount of expected deviation from the cooling curves shown in Fig. 25.3, it is possible to show that they are entirely inconsistent with the notion of reversible adiabatic, i.e., entropy conserving, expansion. As the expansion proceeds along $U = \text{const.}$ lines, we can compute the entropy per participating baryon using Eqs. (27.38) and (27.39), and we find a significant growth of total entropy. As shown in Fig. 27.3b, the entropy rises initially in the dense phase of the matter by as much as 50–100% due to the pion production and resonance decay. Amusingly enough, as the newly produced entropy is carried mostly by pions, one will find that the entropy carried by protons remains constant. With this remarkable behaviour of the entropy, we are in a certain sense, victims of our elaborate theory. Had we used, e.g., an ideal gas of Fermi nucleons, then the expansion would seem to be entropy conserving, as pion production and other chemistry were forgotten. Our fireballs have no tendency to expand reversibly and adiabatically, as many reaction channels are open. A more complete discussion of the entropy puzzle can be found in [1].

Inspecting Fig. 27.2 again, it seems that a possible test of the equations of state for the hadronic gas consists in measuring the temperature in the hot fireball zone, and doing this as a function of the nuclear collision energy. The plausible assumption made is that the fireball follows the ‘cooling’ lines shown in Fig. 27.2 until final dissociation into hadrons. This presupposes that the surface emission of hadrons during the expansion of the fireball does not significantly alter the available energy

per baryon. This is more likely true for sufficiently large fireballs. For small ones, pion emission by the surface may influence the energy balance. As the fireball expands, the temperature falls and the chemical composition changes. The hadronic clusters dissociate and more and more hadrons are to be found in the ‘elementary’ form of a nucleon or a pion. Their kinetic energies are reminiscent of the temperature found at each phase of the expansion.

To compute the experimentally observable final temperature [1, 13], we shall argue that a time average must be performed along the cooling curves. Not knowing the reaction mechanisms too well, we assume that the temperature decreases approximately linearly with the time in the significant expansion phase. We further have to allow that a fraction of particles emitted can be reabsorbed in the hadronic cluster. This is a geometric problem and, in a first approximation, the ratio of the available volume Δ to the external volume V_{ex} is the probability that an emitted particle not be reabsorbed, i.e., that it can escape:

$$R_{\text{esc}} = \frac{\Delta}{V_{\text{ex}}} = 1 - \frac{\varepsilon(\beta, \lambda)}{4\mathcal{B}}. \quad (27.65)$$

The relative emission rate is just the integrated momentum spectrum

$$R_{\text{emis}} = \int \frac{d^3p}{(2\pi)^3} e^{-\sqrt{p^2+m^2}/T+\mu/T} = \frac{m^2 T}{2\pi^2} K_2(m/T) e^{\mu/T}. \quad (27.66)$$

The chemical potential acts only for nucleons. In the case of pions, it has to be dropped from the above expression. For the mean temperature, we thus find

$$\langle T \rangle = \frac{\int_{\text{c}} R_{\text{esc}} R_{\text{emis}} T dT}{\int_{\text{c}} R_{\text{esc}} R_{\text{emis}} dT}, \quad (27.67)$$

where the subscript c on the integral indicates here a line integral along that particular cooling curve in Fig. 27.2 which belongs to the energy per baryon fixed by the experimentalist.

In practice, the temperature is most reliably measured through the measurement of mean transverse momenta of the particles. It may be more practical therefore to calculate the average transverse momentum of the emitted particles. In principle, to obtain this result we have to perform a similar averaging to the one above. For the average transverse momentum at given T, μ , we find [8]

$$\langle p_{\perp}(m, T, \mu) \rangle_p = \frac{\int p_{\perp} e^{-\sqrt{p^2+m^2}-\mu)/T} d^3p}{\int e^{-\sqrt{p^2+m^2}-\mu)/T} d^3p} = \frac{\sqrt{\pi m T / 2} K_{5/2}(m/T) e^{\mu/T}}{K_2(m/T) e^{\mu/T}}. \quad (27.68)$$

The average over the cooling curve is then

$$\langle (p_{\perp}(m, T, \mu))_p \rangle_c = \frac{\int_c \frac{\Delta}{V_{\text{ex}}} T^{3/2} \sqrt{\pi m/2} K_{5/2}(m/T) e^{\mu/T} dT}{\int_c \frac{\Delta}{V_{\text{ex}}} T K_2(m/T) e^{\mu/T} dT} . \quad (27.69)$$

We did verify numerically that the order of averages does not matter:

$$\langle p_{\perp}(m, \langle T \rangle_c, \mu) \rangle_p \approx \langle (p_{\perp}(m, T, \mu))_p \rangle_c , \quad (27.70)$$

which shows that the mean transverse momentum is also the simplest (and safest) method of determining the average temperature (indeed better than fitting ad hoc exponential functions to p_{\perp} distributions).

In the presented calculations, we chose the bag constant $\mathcal{B} = (145 \text{ MeV})^4$, but we now believe that a larger \mathcal{B} should be used. As a consequence of our choice and the measured pion temperature of $\langle T \rangle_{\pi}^{\text{ex}} = 140 \text{ MeV}$ at highest ISR energies, we have to choose the constant H such that $T_0 = 190 \text{ MeV}$ [see Eq. (27.46)].

The average temperature, as a function of the range of integration over T , reaches different limiting values for different particles. The limiting value obtained thus is the observable ‘average temperature’ of the debris of the interaction, while the initial temperature T_{cr} at given $E_{k,\text{lab}}$ (full line in Fig. 27.4) is difficult to observe. When integrating along the cooling line as in Eq. (27.67), we can easily, at each point, determine the average hadronic cluster mass. The integration for protons is interrupted (protons are ‘frozen out’) when the average cluster mass is about half the nucleon isobar mass. We have also considered baryon density dependent freeze-out, but such a procedure depends strongly on the unreliable value of \mathcal{B} .

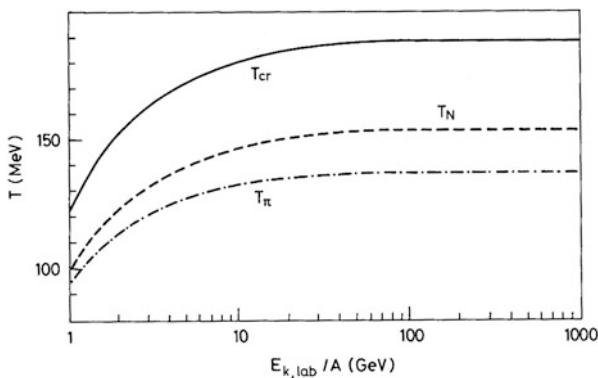
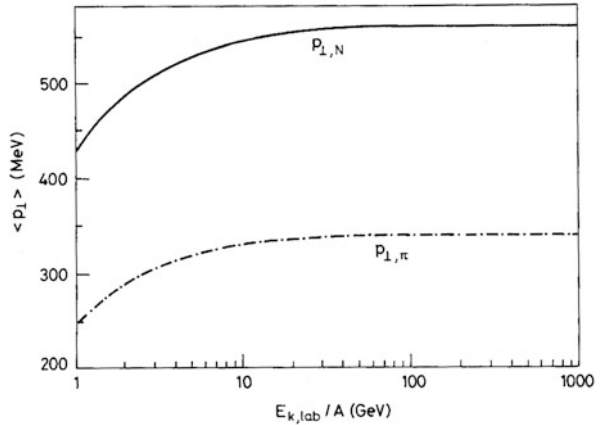


Fig. 27.4 Mean temperatures for nucleons and pions together with the critical temperature belonging to the point where the ‘cooling curves’ start off the critical curve (see Fig. 27.2a). The mean temperatures are obtained by integrating along the cooling curves. Note that T_N is always greater than T_{π}

Fig. 27.5 Mean transverse momenta of nucleons and pions found by integrating along the ‘cooling curves’



Our choice of the freeze-out condition was made in such a way that the nucleon temperature at $E_{k,lab}/A = 1.8$ GeV is about 120 MeV. The model dependence of our freeze-out introduces an uncertainty of several MeV in the average temperature. In Fig. 27.4, the pion and nucleon average temperatures are shown as a function of the heavy ion kinetic energy. Two effects contributed to the difference between the π and N temperatures:

1. The particular shape of the cooling curves (Fig. 27.2a). The chemical potential drops rapidly from the critical curve, thereby damping relative baryon emission at lower T . Pions, which do not feel the baryon chemical potential, continue being created also at lower temperatures.
2. The freeze-out of baryons occurs earlier than the freeze-out of pions.

A third effect has been so far omitted—the emission of pions from two-body decay of long-lived resonances [1] would lead to an effective temperature which is lower in nuclear collisions.

In Fig. 27.5, we show the dependence of the average transverse momenta of pions and nucleons on the kinetic energy of the heavy ion projectiles.

27.6 Strangeness in Heavy Ion Collisions

From the averaging process described here, we have learned that the temperatures and transverse momenta of particles originating in the hot fireballs are more reminiscent of the entire history of the fireball expansion than of the initial hot compressed state, perhaps present in the form of quark matter. We may generalize this result and then claim that most properties of inclusive spectra are reminiscent of the equations of state of the hadronic gas phase and that the memory of the initial

dense state is lost during the expansion of the fireballs as the hadronic gas rescatters many times while it evolves into the final kinetic and chemical equilibrium state.

In order to observe properties of quark-gluon plasma, we must design a thermometer, an isolated degree of freedom weakly coupled to the hadronic matter. Nature has, in principle (but not in practice) provided several such thermometers: leptons and heavy flavours of quarks. We would like to point here to a particular phenomenon perhaps quite uniquely characteristic of quark matter. First we note that, at a given temperature, the quark-gluon plasma will contain an equal number of strange (s) quarks and antistrange (\bar{s}) quarks, naturally assuming that the hadronic collision time is much too short to allow for light flavour weak interaction conversion to strangeness. Thus, assuming equilibrium in the quark plasma, we find the density of the strange quarks to be (two spins and three colours)

$$\frac{s}{V} = \frac{\bar{s}}{V} = 6 \int \frac{d^3p}{(2\pi)^3} e^{-\sqrt{p^2+m_s^2}/T} = 3 \frac{Tm_s^2}{\pi^2} K_2(m_s/T), \quad (27.71)$$

neglecting for the time being the perturbative corrections and, of course, ignoring weak decays. As the mass m_s of the strange quarks in the perturbative vacuum is believed to be of the order of 280–300 MeV, the assumption of equilibrium for $m_s/T \sim 2$ may indeed be correct. In Eq. (27.71), we were able to use the Boltzmann distribution again, as the density of strangeness is relatively low. Similarly, there is a certain light antiquark density (\bar{q} stands for either \bar{u} or \bar{d}):

$$\frac{\bar{q}}{V} = 6 \int \frac{d^3p}{(2\pi)^3} e^{-|p|/T - \mu_q/T} = e^{-\mu_q/T} T^3 \frac{6}{\pi^2}, \quad (27.72)$$

where the quark chemical potential is $\mu_q = \mu/3$, as given by Eq. (27.49). This exponent suppresses the $q\bar{q}$ pair production.

What we intend to show is that there are many more \bar{s} quarks than antiquarks of each light flavour. Indeed,

$$\frac{\bar{s}}{\bar{q}} = \frac{1}{2} \left(\frac{m_s}{T} \right)^2 K_2 \left(\frac{m_s}{T} \right) e^{\mu/3T}. \quad (27.73)$$

The function $x^2 K_2(x)$ is, for example, tabulated in [22]. For $x = m_s/T$ between 1.5 and 2, it varies between 1.3 and 1. Thus, we almost always have more \bar{s} than \bar{q} quarks and, in many cases of interest, $\bar{s}/\bar{q} \sim 5$. As $\mu \rightarrow 0$, there are about as many \bar{u} and \bar{q} quarks as there are \bar{s} quarks.

When the quark matter dissociates into hadrons, some of the numerous \bar{s} may, instead of being bound in a $q\bar{s}$ kaon, enter into a $\bar{q}\bar{q}\bar{s}$ antibaryon and, in particular², a $\bar{\Lambda}$ or $\bar{\Sigma}^0$. The probability for this process seems to be comparable to the similar one for the production of antinucleons by the antiquarks present in the plasma.

² $\bar{\Sigma}^0$ decays into $\bar{\Lambda}$ by emitting a photon and is always counted as part of a $\bar{\Lambda}$ abundance.

What is particularly noteworthy about the \bar{s} -carrying antibaryons is that they can conventionally only be produced in direct pair production reactions. Up to about $E_{k,\text{lab}}/A = 3.5 \text{ GeV}$, this process is very strongly suppressed by energy–momentum conservation because, for free pp collisions, the threshold is at about 7 GeV . We would thus like to argue that a study of the $\bar{\Lambda}$ and $\bar{\Sigma}^0$ in nuclear collisions for $2 < E_{k,\text{lab}}/A < 4 \text{ GeV}$ could shed light on the early stages of the nuclear collisions in which quark matter may be formed.

Let us mention here another effect of importance in this context: the production rate of a pair of particles with a conserved quantum number like strangeness will usually be suppressed by the Boltzmann factor $e^{-2m/T}$, rather than a factor $e^{-m/T}$ as is the case in thermomechanical equilibrium (see, for example, the addendum in [8]). As relativistic nuclear collisions are just on the borderline between those two limiting cases, it is important when considering the yield of strange particles to understand the transition between them. We will now show how one can describe these different cases in a unified statistical description [23].

As we have already implicitly discussed [see Eq. (27.13)], the logarithm of the grand partition function Z is a sum over all different particle configurations, e.g., expressed with the help of the mass spectrum. Hence, we can now concentrate in particular on that part of $\ln Z$ which is exclusively associated with the strangeness.

As the temperatures of interest to us and which allow appreciable strangeness production are at the same time high enough to prevent the strange particles from being thermodynamically degenerate, we can restrict ourselves again to the discussion of Boltzmann statistics only.

The contribution to Z of a state with k strange particles is

$$Z_k = \frac{1}{k!} \left[\sum_s Z_1^s(T, V) \right]^k, \quad (27.74)$$

where the one-particle function Z_1 for a particle of mass m_s is given in Eq. (27.17). To include both particles *and* antiparticles as two thermodynamically independent phases in Eq. (27.74), the sum over s in Eq. (27.74) must include them both. As the quantum numbers of particles (p) and antiparticles (a) must always be present with *exactly* the same total number, not each term in Eq. (27.74) can contribute. Only when $n = k/2 = \text{number of particles} = \text{number of antiparticles}$ is exactly fulfilled do we have a physical state. Hence,

$$Z_{2n}^{\text{pair}} = \frac{1}{(2n)!} \binom{2n}{n} \left(\sum_{s_p} Z_1^{s_p} \right)^n \left(\sum_{s_a} Z_1^{s_a} \right)^n. \quad (27.75)$$

We now introduce the fugacity factor f^n to be able to count the number of strange pairs present. Allowing an arbitrary number of pairs to be produced, we obtain

$$Z_s(\beta, V; f) = \sum_{n=0}^{\infty} \frac{f^n}{n!n!} \left(\sum_{s_p} Z_1^{s_p} \right)^n \left(\sum_{s_a} Z_1^{s_a} \right)^n = I_0(\sqrt{4y}), \quad (27.76)$$

where I_0 is the modified Bessel function and

$$y = f \left(\sum_{s_p} Z_1^{s_p} \right) \left(\sum_{s_a} Z_1^{s_a} \right). \quad (27.77)$$

We have to maintain the difference between the particles (p) and antiparticles (a), as in nuclear collisions the symmetry is broken by the presence of baryons and there is an associated need for a baryon fugacity (chemical potential μ) that controls the baryon number. We obtain

$$Z_1^{p,a} := \sum_{s_{p,a}} Z_1^{s_{p,a}} = \frac{VT^3}{2\pi^2} \left\{ 2W(x_K) + 2e^{\pm\mu/T} [W(x_\Lambda) + 3W(x_\Sigma)] \right\}, \quad (27.78)$$

for particles ($+\mu$) and antiparticles ($-\mu$), where $W(x) = x^2 K_2(x)$, $x_i = m_i/T$, and all kaons and hyperons are counted. In the quark phase, we have

$$Z_{1,q}^{p,a} = \frac{VT^3}{2\pi^2} \left[6 e^{\pm\mu/3T} W(x_s) \right], \quad (27.79)$$

with $Tx_s = m_s \sim 280$ MeV. We note in passing that the baryon chemical potential cancels out in y of Eq. (27.77) when Eq. (27.79) is inserted in the quark phase [compare with Eq. (27.71)].

By differentiating $\ln Z_s$ of Eq. (27.76) with respect to f , we find the strangeness number present at given T and V :

$$\langle n \rangle_s = f \frac{\partial}{\partial f} \ln Z_s \Big|_{f=1} = \frac{I_1(\sqrt{4y})}{I_0(\sqrt{4y})} \sqrt{y}. \quad (27.80)$$

For large y , that is, at given T for large volume V , we find $\langle n \rangle_s = \sqrt{y} \sim e^{-m/T}$, as expected. For small y , we find $\langle n \rangle_s = y \sim e^{-2m/T}$. In Fig. 27.6, we show the dependence of the quenching factor $I_1/I_0 = \eta$ as a function of the volume V measured in units of $V_h = 4\pi/3 \text{ fm}^3$ for a typical set of parameters: $T = 150$, $\mu = 550$ MeV (hadronic gas phase).

The following observations follow from inspection of Fig. 27.6:

1. The strangeness yield is a qualitative measure of the hadronic volume in thermodynamic equilibrium.

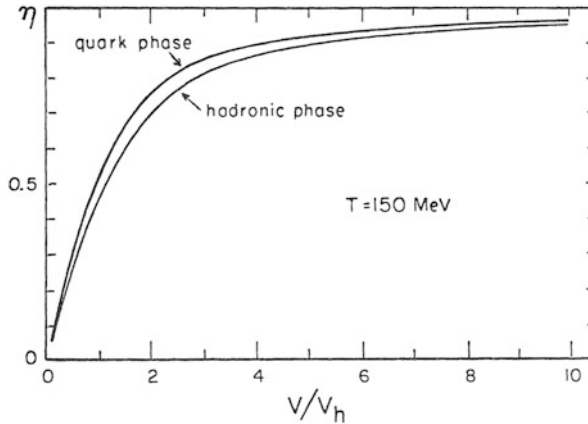


Fig. 27.6 The quenching factor for strangeness production as a function of the active volume V/V_h , where $V_h = 4\pi/3 \text{ fm}^3$, the hadron curve was obtained for baryochemical potential $\mu = 550 \text{ MeV}$

2. Total strangeness yield is not an indicator of the phase transition to quark plasma, as the enhancement ($\sqrt{\eta_q/\eta} = 1.25$) in yield can be reinterpreted as being due to a change in hadronic volume.
3. We can expect that, in nuclear collisions, the active volume will be sufficiently large to allow the strangeness yield to correspond to that of 'infinite' volume for reactions triggered on 'central collisions'. Hence, e.g., Λ production rate will significantly exceed that found in pp collisions.

Our conclusions about the significance of $\bar{\Lambda}$ as an indicator of the phase transition to quark plasma remain valid as the production of $\bar{\Lambda}$ in the hadronic gas phase will only be possible in the very first stages of the nuclear collisions, if sufficient centre of mass energy is available.

27.7 Summary

Our aim has been to obtain a description of hadronic matter valid for high internal excitations. By postulating the kinetic and chemical equilibrium, we have been able to develop a thermodynamic description valid for high temperatures and different chemical compositions. In our work we have found two physically different domains: firstly, the hadronic gas phase, in which individual hadrons can exist as separate entities, but are sometimes combined into larger hadronic clusters, while in the second domain, individual hadrons dissolve into one large cluster consisting of hadronic constituents, viz., the quark-gluon plasma.

In order to obtain a theoretical description of both phases, we have used some 'common' knowledge and plausible interpretations of currently available

experimental observations. In particular, in the case of hadronic gas, we have completely abandoned a more conventional Lagrangian approach in favour of a semi-phenomenological statistical bootstrap model of hadronic matter that incorporates those properties of hadronic interaction that are, in our opinion, most important in nuclear collisions.

In particular, the attractive interactions are included through the rich, exponentially growing hadronic mass spectrum $\tau(m^2, b)$, while the introduction of the finite volume of each hadron is responsible for an effective short-range repulsion. Aside from these manifestations of strong interactions, we only satisfy the usual conservation laws of energy, momentum, and baryon number. We neglect quantum statistics since quantitative study has revealed that this is allowed above $T \approx 50$ MeV. But we allow particle production, which introduces a quantum physical aspect into the otherwise ‘classical’ theory of Boltzmann particles.

Our approach leads us to the equations of state of hadronic matter which reflect what we have included in our considerations. It is the *quantitative* nature of our work that allows a detailed comparison with experiment. This work has just begun and it is too early to say if the features of strong interactions that we have chosen to include in our considerations are the most relevant ones. It is important to observe that the currently predicted pion and nucleon mean transverse momenta and temperatures show the required substantial rise (see Fig. 27.5) as required by the experimental results available at $E_{k,\text{lab}}/A = 2$ GeV (BEVALAC, see [19]) and at 1,000 GeV (ISR, see [18]). Further comparisons involving, in particular, particle multiplicities and strangeness production are under consideration.

We also mention the internal theoretical consistency of our two-fold approach. With the proper interpretation, the statistical bootstrap leads us, in a straightforward fashion, to the postulate of a phase transition to the quark-gluon plasma. This second phase is treated by a quite different method. In addition to the standard Lagrangian quantum field theory of weakly interacting particles at finite temperature and density, we also introduce the phenomenological vacuum pressure and energy density \mathcal{B} .

Perhaps the most interesting aspect of our work is the realization that the transition to quark matter will occur at much lower baryon density for highly excited hadronic matter than for matter in the ground state ($T = 0$). The precise baryon density of the phase transition depends somewhat on the bag constant, but we estimate it to be at about $2-4\nu_0$ at $T = 150$ MeV. The detailed study of the different aspects of this phase transition, as well as of possible characteristic signatures of quark matter, must still be carried out. We have given here only a very preliminary report on the status of our present understanding.

We believe that the occurrence of the quark plasma phase is observable and we have proposed therefore a measurement of the $\bar{\Lambda}/\bar{p}$ relative yield between 2 and 10 GeV/ N kinetic energies. In the quark plasma phase, we expect a significant enhancement of $\bar{\Lambda}$ production which will most likely be visible in the $\bar{\Lambda}/\bar{p}$ relative rate.

Acknowledgements Many fruitful discussions with the GSI/LBL Relativistic Heavy Ion group stimulated the ideas presented here. I would like to thank R. Bock and R. Stock for their hospitality at GSI during this workshop. As emphasized before, this work was performed in collaboration with R. Hagedorn.

Open Access This book is distributed under the terms of the Creative Commons Attribution Non-commercial License which permits any noncommercial use, distribution, and reproduction in any medium, provided the original author(s) and sources are credited.

References

1. R. Hagedorn, J. Rafelski, Manuscript in preparation for Physics Reports (This manuscript was never completed, the present volume comprises most if not all material that would have been included.); see also, preprints CERN-TH-2947 and CERN-TH-2969 From hadron gas to quark matter I & II, in the *Proceedings of the International Symposium on Statistical Mechanics of Quarks and Hadrons*, Bielefeld, Germany, August 1980, ed. by H. Satz (North Holland, Amsterdam, 1980)
2. The many-body theory for QCD at finite temperatures has been discussed in:
B.A. Freedman, L.D. McLerran, *Phys. Rev. D* **16**, 1169 (1977);
P.D. Morley, M.B. Kislinger, *Phys. Rep.* **51**, 63 (1979);
J.I. Kapusta, *Nucl. Phys. B* **148**, 461 (1979);
E.V. Shuryak, *Phys. Lett. B* **81**, 65 (1979); E.V. Shuryak, *Phys. Rep.* **61**, 71 (1980);
O.K. Kalashnikov, V.V. Klimov, *Phys. Lett. B* **88**, 328 (1979)
3. B. Touschek, *Nuovo Cimento B* **58**, 295 (1968)
4. W. Marciano, H. Pagels, *Phys. Rep.* **36**, 137 (1978)
5. K. Johnson, The MIT bag model. *Acta Phys. Polon. B* **6**, 865 (1975)
6. A. Chodos, R.L. Jaffe, K. Johnson, C.B. Thorn, V.F. Weisskopf, *Phys. Rev. D* **9**, 3471 (1974)
7. R. Hagedorn, *Suppl. Nuovo Cimento* **3**, 147 (1965)
8. R. Hagedorn, *Lectures on the Thermodynamics of Strong Interactions*. CERN Yellow Report 71-12 (1971)
9. R. Hagedorn, I. Montvay, J. Rafelski, *Lecture at Erice workshop, Hadronic Matter at Extreme Energy Density*, ed. by N. Cabibbo, L. Sertorio (Plenum Press, New York, 1980), p. 49; and see Chap. 23 in this volume.
10. R. Hagedorn, How to deal with relativistic heavy ion collisions, preceding Chapter 26 in this volume.
11. H. Grote, R. Hagedorn, J. Ranft, *Atlas of Particle Production Spectra* (CERN, Geneva, 1970)
12. J. Rafelski, H.Th. Elze, R. Hagedorn, in *Proceedings of the Fifth European Symposium on Nucleon-Antinucleon Interactions*, Bressanone, June 1980, ed. by M. Cresti (CLEUP publishers, Padova), p. 357 [CERN preprint TH 2912 (August 1980)]
13. R. Hagedorn, J. Rafelski, *Phys. Lett. B* **97**, 136 (1980)
14. F. Karsch, H. Satz, *Phys. Lett.* **21**, 1168 (1980) [The ‘solidification’ of hadronic matter, a purely geometric effect, discussed in this reference should not be confused with the transition to the quark plasma phase discussed here]
15. R. Hagedorn and J. Rafelski: *Commun. Math. Phys.* **83**, 563 (1982)
16. S. Frautschi, *Phys. Rev. D* **3**, 2821 (1971)
17. R. Hagedorn, I. Montvay, *Nucl. Phys. B* **59**, 45 (1973)
18. G. Giacommelli, M. Jacob, *Phys. Rep.* **55**(1), 1 (1979)
19. A. Sandoval, R. Stock, H.E. Stelzer, R.E. Renfordt, J.W. Harris, J. Brannigan, J.B. Geaga, L.J. Rosenberg, L.S. Schroeder, K.L. Wolf, *Phys. Rev. Lett.* **45**, 874 (1980)

20. R. Hagedorn, J. Ranft, Suppl. Nuovo Cimento **6**, 169 (1968);
W.D. Myers, Nucl. Phys. A **296**, 177 (1978);
J. Gosset, J.L. Kapusta, G.D. Westfall, Phys. Rev. C **18**, 844 (1978);
R. Malfliet, Phys. Rev. Lett. **44**, 864 (1980)
21. The possible formation of quark-gluon plasma in nuclear collisions was first discussed quantitatively by
S.A. Chin, Phys. Lett. B **78**, 552 (1978);
see also N. Cabibbo, G. Parisi, Phys. Lett. B **59**, 67 (1975)
22. M. Abramowitz, I.A. Stegun (eds.), *Handbook of Mathematical Functions* (NBS, Washington, 1964)
23. J. Rafelski, M. Danos, Phys. Lett. B **97**, 279 (1980)